Characterization of molybdenum-containing catalysts by ^{95}Mo solid-state NMR

Spectroscopic background: ^{95}Mo nuclei have a spin of I = 5/2 and a quadrupole moment of Q = -2.2 x 10^{-30} m^2. Therefore, ^{95}Mo NMR signals of molybdenum atoms in solids are affected by quadrupolar interactions. Due to the large electron valence shells of molybenum atoms, the anisotropic chemical shielding is an additional strong solid-state interaction. The ^{95}Mo isotope has a natural abundance of 15.90 %, a resonance frequency of ν_0 = 32.59 MHz at B_0 = 11.75, and a sensitivity of 3.3 x 10^{-3} in comparison with ^{1}H nuclei (1.0). Since the ^{97}Mo isotope (spin I = 5/2, ν_0 = 33.28 MHz at B_0 = 11.75) has a natural abundance of 9.56 % only, the ^{95}Mo isotope is the most suitable candidate for NMR studies of molybdenum in solids. Often, the low resonance frequency of ^{95}Mo nuclei is not in the range of standard solid-state NMR probes. In this case, a specific low-frequency NMR probe is required for ^{95}Mo solid-state NMR investigations. For basic principles of solid-state NMR, see lectures “Solid-State NMR Spectroscopy” for Bachelor students or PhD seminars, accessible via the link “Lectures for Students”.

Early ^{95}Mo solid-state NMR studies focused on molybdenum-containing crystalline materials and were performed in a magnetic field of B_0 = 9.4 T [1-4]. For this purpose, static quad-echo NMR spectra or single pulse-excited MAS NMR spectra were recorded. With the availability of high-field and ultra-high-field NMR spectrometers, ^{95}Mo solid-state NMR studies were performed in magnetic fields of B_0 = 18.8 [5], 19.6 T [6], 21.1 T [7], 28.2 [8], and 35.2 T [9].

For an overview on the ^{95}Mo NMR parameters of various tetrahedral coordination compounds and octahedral structures, see Ref. [6]. Generally, molybdenum species have quadrupole coupling constants, e.g., of up to C_Q = 5 MHz for MoO_3 [6, 10], while the isotropic chemical shifts cover a large range, e.g. of δ_{iso} = -1850 ppm for $Mo(CO)_6$ [1], -73 to -20 ppm for MoO_3 [6, 10], and 205 ppm for $[(NH_4)_6Mo_7O_{24}]\cdot 4H_2O$ (type III) [6]. Due to the large number electrons of molybdenum atoms, also a large range of chemical shift anisotropies occurs, e.g. of $\Delta\sigma_{aniso}$ = -400 ppm for $(NtBu_4)_2Mo_6O_{19}$ [6] up to 260 ppm for MoO_3 [6].

As an example, **Figs. 1a and 1b** show the static ^{95}Mo quad-echo NMR spectrum and the ^{95}Mo MAS NMR spectrum of **hexacarbonylmolybdenum ($Mo(CO)_6$)**, recorded at B_0 = 9.4 T [1]. The upper inset in **Fig. 1a** is an expansion of the central transition,

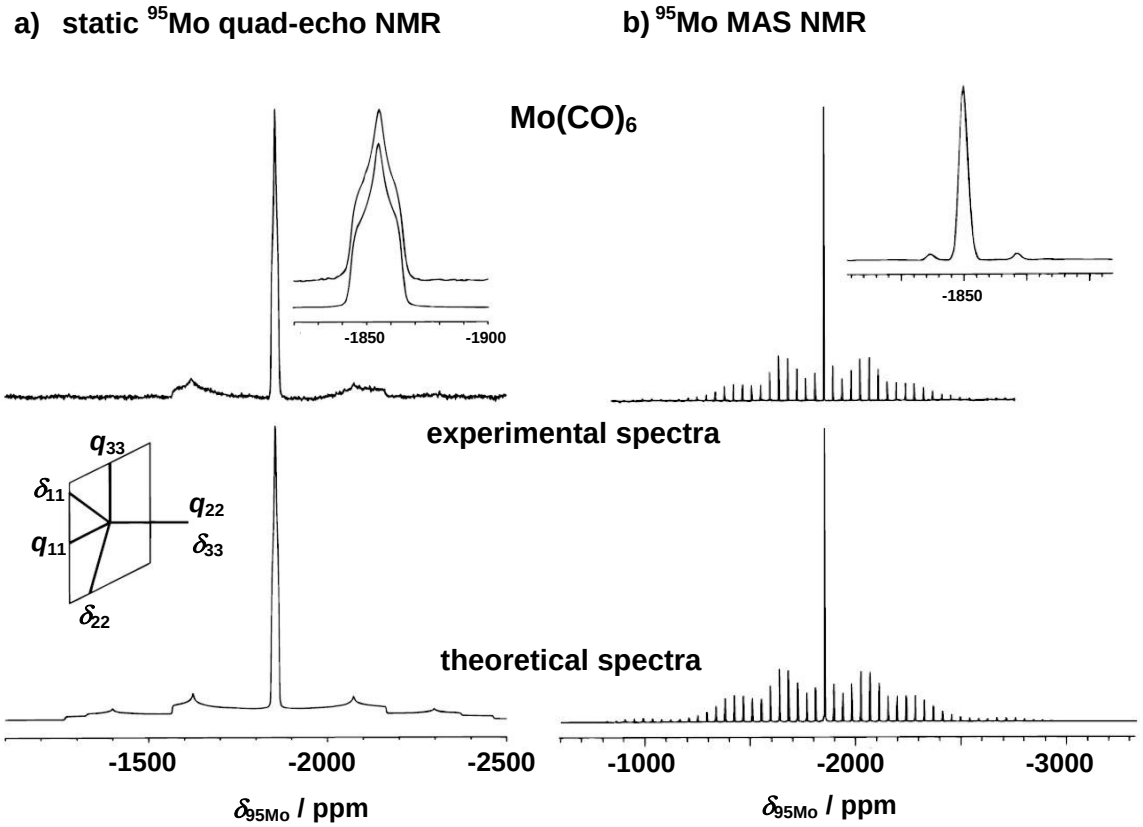

Fig. 1

which shape is affected by the anisotropic chemical shielding interaction of the ^{95}Mo nuclei. The lower inset indicates the relative orientation of the molybdenum chemical shift and electric field gradient tensors with the principal components δ_{11}, δ_{22}, δ_{33} and q_{11}, q_{22}, q_{33}, respectively. Weak symmetric signals in the quad-echo NMR spectrum are due to satellite transitions.

The inset in **Fig. 1b** is an expansion of the central line with ^{13}C satellites, arising from an indirect ^{95}Mo-^{13}C spin-spin coupling, $^{1}J(^{95}\text{Mo},^{13}\text{C})$, of ca. 70 Hz. Due to the low sample spinning rate of ν_{rot} = 1122 Hz and because of the low ^{95}Mo quadrupole coupling constant of C_{Q} = 91 kHz [1], the satellite transitions can be well observed via the envelope of the MAS NMR spinning sidebands. In the case of significantly larger quadrupole coupling constants of ^{95}Mo nuclei in solids, the **observation of the complete quad-echo NMR spectrum may be strongly limited by the low signal-to-noise ratio**.

To overcome the problem of low signal-to-noise ratios of broad signals in static quad-echo NMR spectra of ^{95}Mo nuclei with large quadrupole coupling constants, the **QCPMG (quadrupolar Carr-Purcell-Meiboom-Gill) pulse sequence** is utilized [11,

12]. A further improvement was reached by combination of the QCPMG pulse sequence with **WURST (wideband uniform-rate smooth truncation) pulses** [13], which is well-known as WURST-QCPMG experiment [14].

The QCPMG pulse sequence in **Fig. 2a, top,** for sensitivity-enhanced quad-echo NMR of half-integer quadrupolar nuclei consists at first of a standard quad-echo sequence with an optimized τ_2 that the acquisition starts at the echo maximum [11]. The subsequent part accomplishes sampling of the spin-echoes generated by the interrupting train of π refocusing pulses. The receiver-off periods τ_3 and τ_4 serve to protect the receiver from the effects of the π pulses. It is noted that the flip angles of all pulses correspond to the angles effective for selective operation on the {-1/2 ⇔ 1/2} central transition. Thus, for half-integer quadrupolar nuclei with spin I, the flip angles should be reduced by a factor 1/(I+1/2) in the limit of large quadrupole coupling constants [11]. Fourier transformation of the echo train (**Fig. 2a, bottom**) delivers an NMR spectrum, which consists of narrow spikelets, collecting the signal intensities between the spikelets (see **Fig. 3**), like in an MAS sideband pattern, caused by the MAS echoes in the free induction decay. Therefore, the envelope of the spikelets has a much higher signal-to-noise ratio compared with a common quad-echo NMR spectrum.

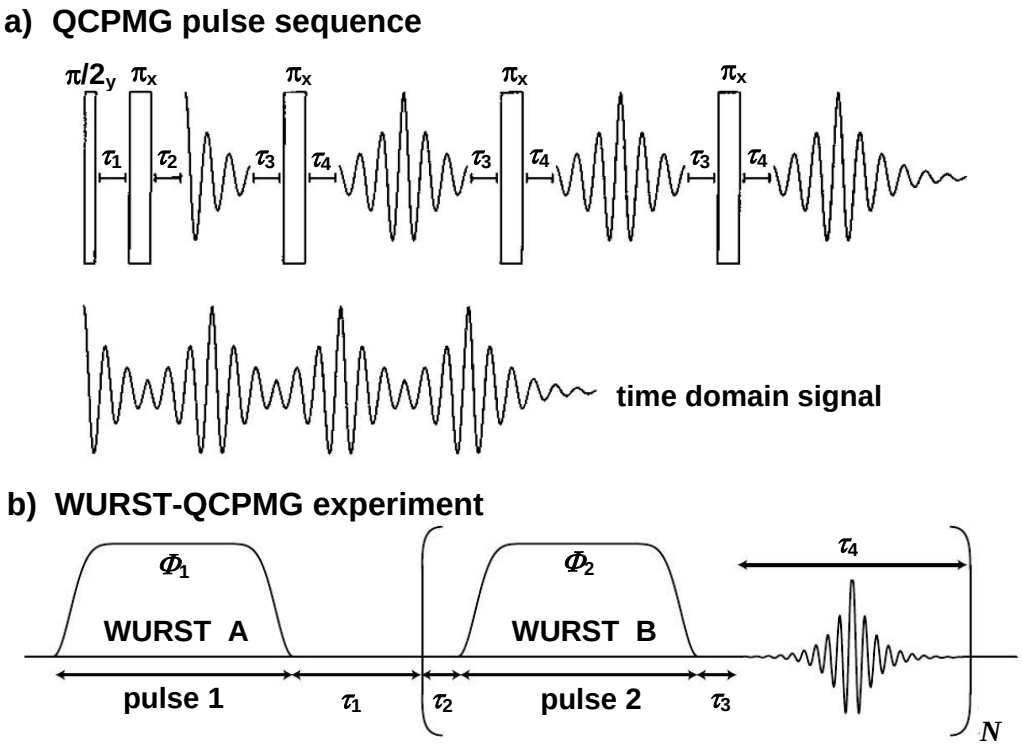

Fig. 2

The WURST-QCPMG experiment in **Fig. 2b** is a frequency-swept echo pulse sequence with a Meiboom-Gill loop placed around the refocusing pulse and acquisition period, analogous to the regular QCPMG experiment. The delays τ_2 and τ_3 are included in the repeating loop for switching between transmission and acquisition modes. The WURST A pulse is an excitation pulse whose frequency is swept adiabatically between positive and negative offset frequencies at a constant rate. These offsets do not necessarily have to be equal. The WURST B pulse is a refocusing π pulse, again swept at a constant rate between positive and negative offsets. Each spectrum is acquired twice, with opposite frequency sweep directions in the second experiment. The two spectra are co-added to compensate for lineshape distortion due to the occurrence of transverse relaxation over the duration of the frequency-dispersed echoes [13]. As an example, **Fig. 3** shows the experimental and deconvoluted **static ^{95}Mo WURST-QCPMG NMR spectra of pure MoO_3 and MoO_2**, respectively, recorded at the resonance frequencies of ν_0 = 52.15 MHz in a magnetic field of B_0 = 18.8 T (see Fig. S6 of Ref. [10]). While the spikelets in the spectrum of MoO_3 describe a single quadrupolar pattern at δ_{iso} = -20 ppm with C_Q = 5 MHz (**Fig. 3a**), two quadrupolar patterns at δ_{iso} = -2100 ppm with C_Q = 2 MHz (blue) and at δ_{iso} = -2900 ppm with C_Q = 22 MHz (violet) can be well-observed in the spectrum of MoO_2 (**Fig. 3b**) [10].

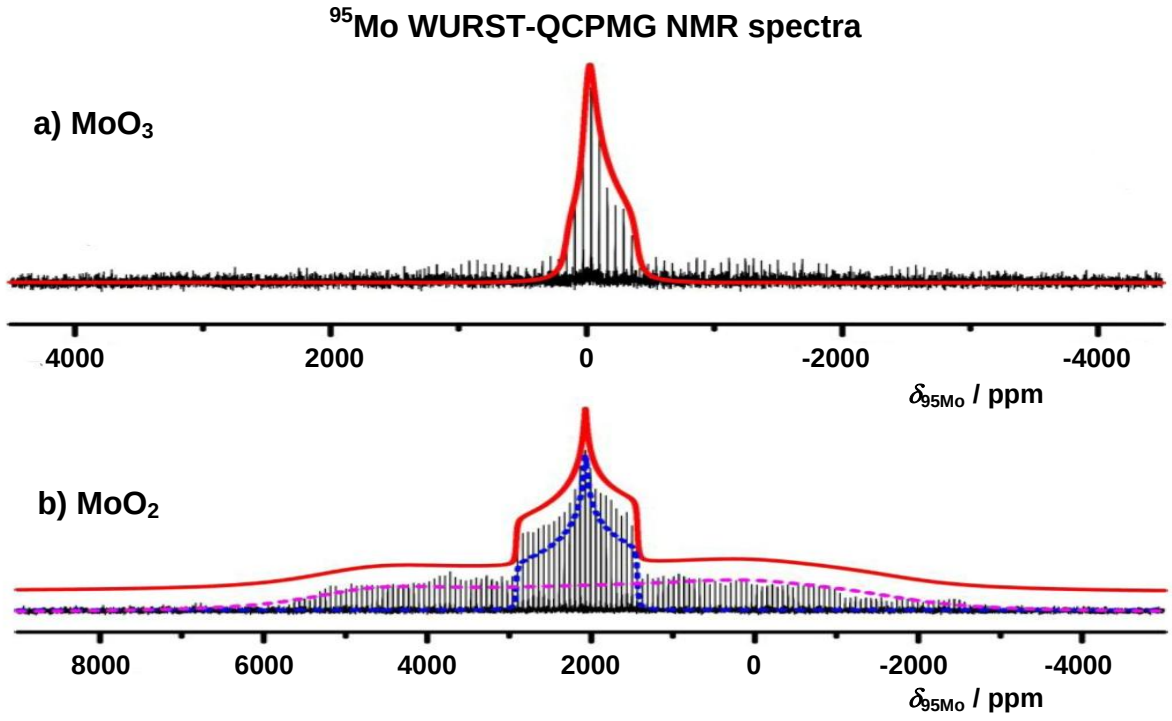

Fig. 3

In the research field of heterogeneous catalysis, ^{95}Mo solid state NMR spectroscopy was utilized, e.g., for the investigation of hydrodesulfurization (HDS) catalyst precursors formed by adsorption of polyoxomolybdates onto γ-alumina and corresponding model compounds via common quad-echo and MAS NMR experiments [3, 4] and of silica supported Mo-based olefin metathesis catalysts via ^{95}Mo QCPMG MAS NMR experiments [8].

The largest number of ^{95}Mo solid-state NMR studies in this research field focused on the investigation of **Mo-containing H-ZSM-5 zeolites for the methane dehydroaromatization (MDA)** [9, 10, 15-18]. These catalysts were prepared by physical mixture of zeolite H-ZSM-5 and MoO_3 (4 wt.%) [17], impregnation of zeolite H-ZSM-5 with ammonium heptamolybdate tetrahydrate (AHM) [17], impregnation of H-ZSM-5 with ^{95}Mo-enriched (94.8 %) molybdenum acetate (MoAC) [15, 16], or dissolution of dispersed ^{95}Mo-enriched (94.8 %) MoO_3 in ammonium hydroxide, utilized for the impregnation of zeolite H-ZSM-5 [9, 10, 18]. Finally, these materials were calcined at temperatures of T = 753 K [15, 16], 773 K [17], or 823 K [9, 10, 18].

Static ^{95}Mo quad-echo NMR and common ^{95}Mo MAS NMR studies of Mo/ZSM-5, prepared by impregnation with ^{95}Mo-enriched MoAC and performed at B_0 = 21.1 T, yielded structure-less signals, explained by a superposition of a narrow component, due to MoO_3, and a broad component, caused by dispersed MoO_x species, introduced into zeolite H-ZSM-5 by Mo exchange [15, 16]. For the latter component, a heterogeneous line broadening was assumed as the dominant mechanism. Saturation-recovery experiments indicated a lattice relaxation time of **$T_1 \leq$ 100 ms for the zeolitic MoO_x species** introduced by Mo exchange, in contrast to a component with **$T_1 \cong$ 30 s, explained by MoO_3 species** [16]. By evaluating the contents of Mo atoms with $T_1 \leq$ 100 ms (MoO_x species) for a homologous series of Mo/H-ZSM-5 zeolites with different Mo loadings, a correlation with the aromatics formation rate during the methane dehydroaromatization (MDA) reaction was obtained [16].

In Ref. [10], **static ^{95}Mo WURST-QCPMG NMR spectroscopy** was utilized for investigating the influence of the MDA reaction on the nature of different MoO_3 and MoO_x species in zeolites Mo/H-ZSM-5. The static ^{95}Mo WURST-QCPMG NMR spectrum of the fresh Mo/ZSM-5 zeolite in **Fig. 4a** was explained by a broad down-field signal (δ_{iso} = -20 ppm, C_Q = 5 MHz, red dashed) due to MoO_3 particles on the external surface of zeolite and a weak up-field signal (δ_{iso} = -165 ppm, C_Q = 5 MHz, tangerine dashed), due to **MoO_x species formed by replacing the acidic protons**

in the zeolite channels of zeolite H-ZSM-5 by Mo exchange [10]. After 5 min of the MDA reaction (**Fig. 4b**), a broad ^{95}Mo WURST-QCPMG NMR signal appeared at δ_{iso} = -2200 ppm (blue dashed), due to the formation of MoO_2 formed by the reduction of MoO_3 clusters by methane. While the unresolved signal in the region of δ_{iso} = -600 to 400 ppm may include contributions from various Mo species, such as **surface MoO_3** clusters, **exchanged MoO_x species**, and partially **carbonized Mo_xC_y species**. The MoO_2 signal disappeared upon a MDA reaction time of 10 min (**Fig. 4c**) and a much broader signal at δ_{iso} = - 280 ppm with C_Q = 15.0 MHz (purple dashed) resembling that of Mo_2C crystallites became dominant. The formation of reduced Mo and carbonized Mo species provided a reasonable explanation for the different reduction steps, found by MS experiments [10]. In the further progress of the MDA reaction

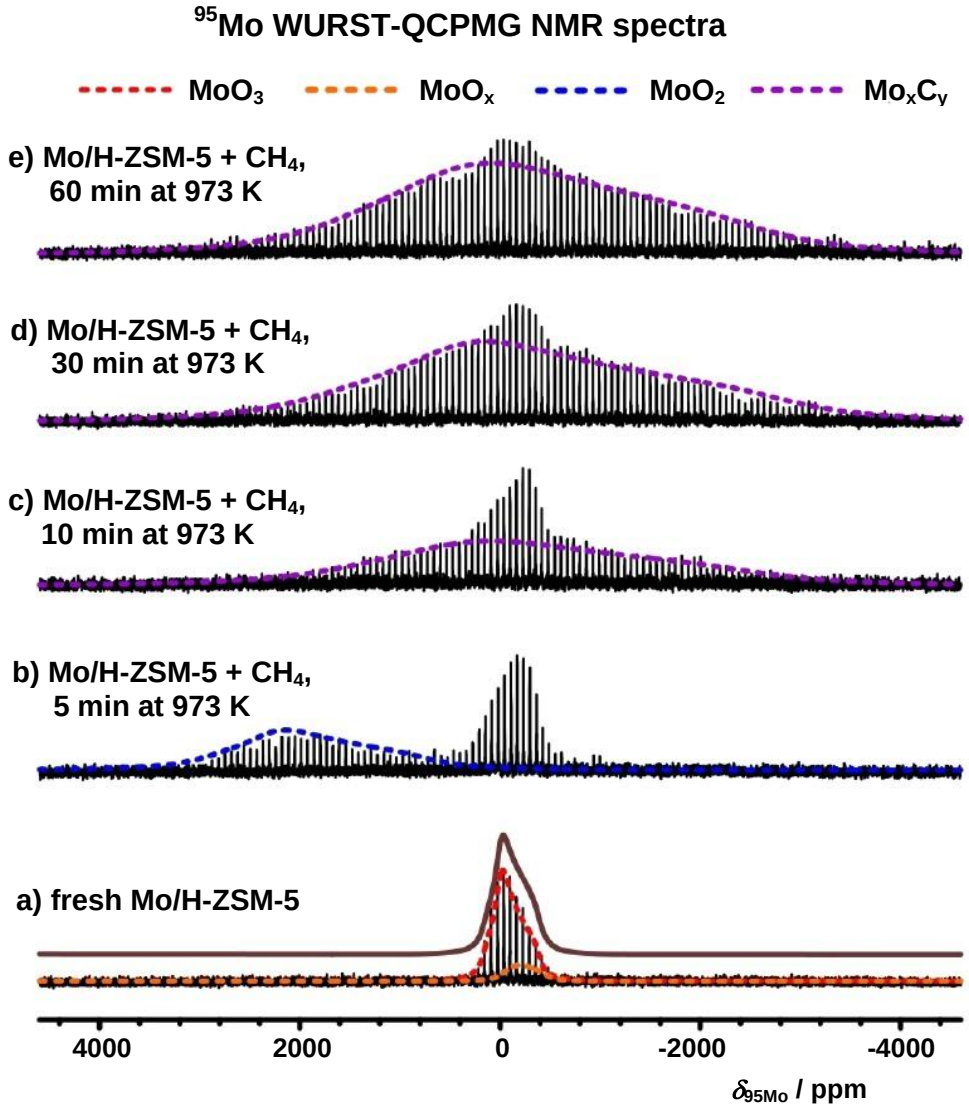

Fig. 4

(**Figs. 4d and 4e**), the broad signal increased due to the gradual accumulation of inactive Mo_xC_y on the external surface of the zeolite Mo/H-ZSM-5 [10].

By **2D ^{1}H{^{95}Mo} population transfer dipolar mediated heteronuclear multiple quantum coherence (PT D-HMQC) NMR** spectroscopy [19, 20], Mo species in the vicinity of protons, within a distance of few angstroms, can be detected. This NMR experiment excludes Mo species located on the external zeolite surface, far away of the active sites, due to their larger distance from protons.

The pulse sequence of the **PT D-HMQC NMR** experiment is shown in **Fig. 5** [20]. This sequence allows the correlation of the NMR signals of spin I nuclei (e.g. ^{31}P or ^{1}H) with the transitions of quadrupolar nuclei with spin S (e.g. ^{27}Al or ^{95}Mo). The coherences of spins S are excited and reconverted using central transition selective $\pi/2$-pulses. MAS averages out the anisotropic NMR interactions and the evolution under the isotropic chemical shift of the spin I nuclei is refocused by the middle π pulse. The isotropic shift of spin S nuclei is encoded by the evolution of the multiple-quantum coherences during the period t_1. The evolution of dipolar coupling during t_1 is cancelled by the π pulse in the spin I channel. By applying WURST pulses during the τ_{mix} delays, a continuous saturation of the spin S transitions is achieved, which accelerates the population transfer. For further details, see Ref. [20]. In this reference, the above-mentioned pulse experiment was utilized for ^{31}P{^{27}Al} PT D-HMQC studies of an APO_4-14 material.

PT D-HMQC NMR experiment

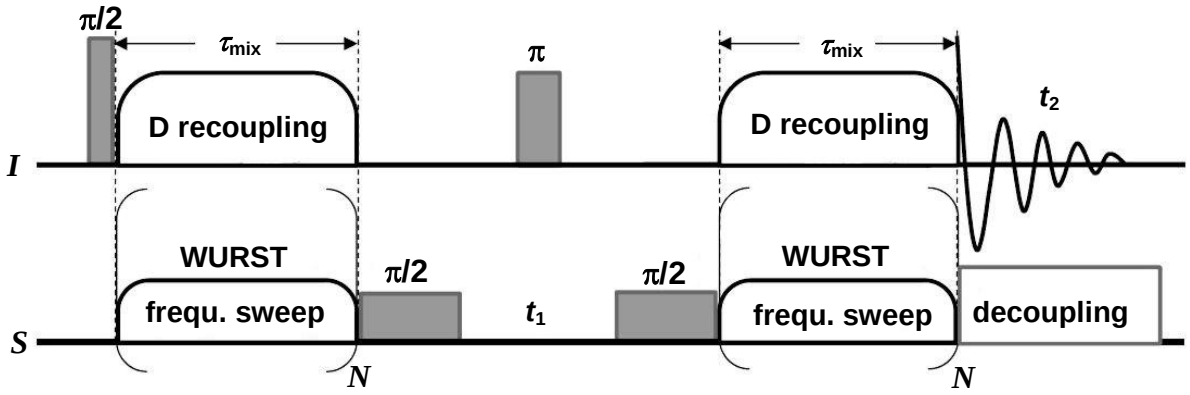

Fig. 5

The two-dimensional (2D) ^{1}H{^{95}Mo} PT D-HMQC NMR spectrum of fresh Mo/H-ZSM-5 zeolite (^{95}Mo-enriched, 94.8 %) in **Fig. 6a** was recorded in a magnetic field of B_0 =

9.4 T [18]. This 2D spectrum shows ^{1}H-^{95}Mo correlations between exchanged Mo-oxo (MoO_x in Ref. [10]) species (δ_{iso} = -165 ppm) and protons from both the Broensted acidic (BAS) bridging OH groups at δ_{1H} = 4.0 ppm and AlOH groups at δ_{1H} = 2.6 ppm in the zeolite channels. The exchanged Mo-oxo species anchored on the BASs of zeolite H-ZSM-5 are recognized as precursors for the catalytically active sites. After a MDA reaction time of 30 min (**Fig. 6b**) [18], ^{1}H-^{95}Mo correlations for **Mo carbide species, named as MoO_xC_y-1, at δ_{iso} ≈ -84 ppm and a second one, named as MoO_xC_y-2, at δ_{iso} ≈ -48 ppm** occur. These correlations indicate an evolution of the Mo species in the zeolite channels, where the exchanged Mo-oxo species on the BASs are partially reduced by methane to Mo carbide species and

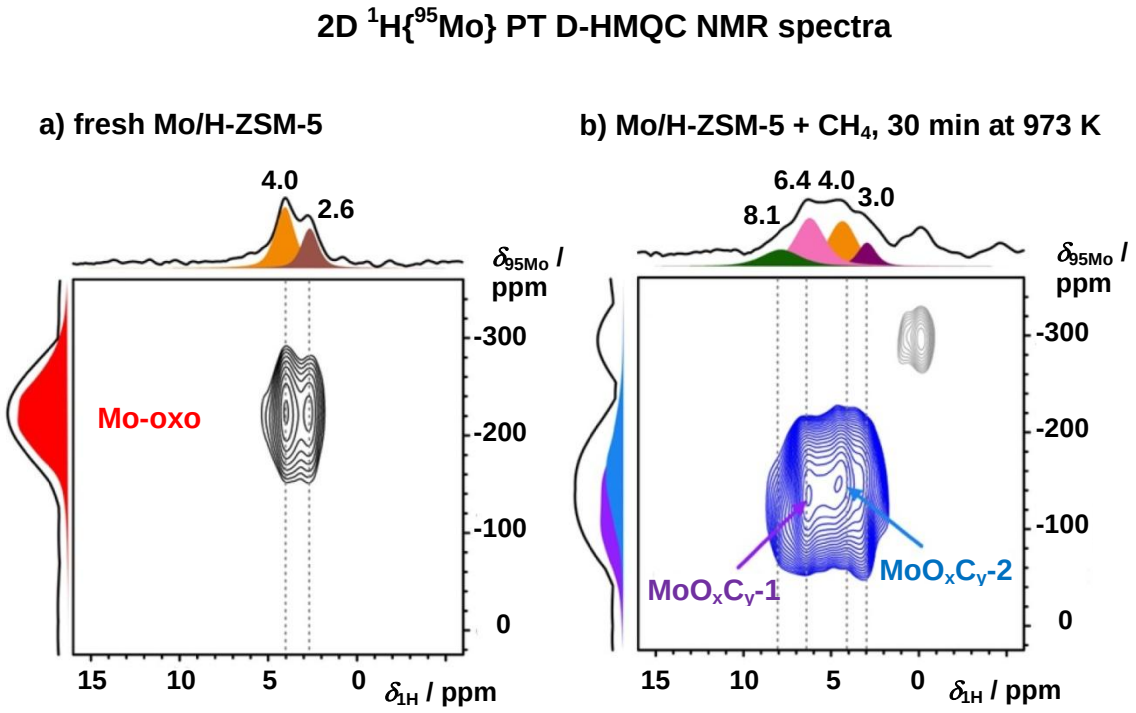

Fig. 6

H_2O. The formation of these carbide species is accompanied by ^{1}H NMR signals of trapped olefins at δ_{1H} = 6.4 ppm and aromatics at δ_{1H} = 8.1 ppm [18].

In **Table 1**, a survey on the ^{95}Mo solid-state NMR parameters of above-mentioned and additional materials, mostly determined by static ^{95}Mo WURST-QCPMG NMR, is given. See Tables in the Supporting Information of the references in the last column.

Materials and Mo Species	C_Q / MHz	η_Q	δ_{iso} / ppm	Refs.
$Mo(CO)_6$, pure	0.09	0.14	-1854	[1]
$[(NH_4)_6Mo_7O_{24}]\cdot 4H_2O$ (type III)	3.0		205	[6]
MoO_3, pure	5.0 ± 0.5	0.9 to 1.0	-20 ± 2	[10], [18]
MoO_2, pure	2.0 ± 0.2	0.9 to 1.0	2100 ± 100	[10]
	22.0 ± 2.0	0.0 to 0.3	2900 ± 100	[10]
Mo_2C, pure	18.0 ± 1.0	0.8 to 1.0	600 ± 50	[10]
MoO_3 on Mo/H-ZSM-5	5.0 ± 0.5	0.9 to 1.0	-20 ± 2	[18]
MoO_2 on Mo/H-ZSM-5	10.0 ± 1.0	0.9 to 1.0	2200 ± 50	[18]
MoO_x, Mo-oxo, on Mo/H-ZSM-5	5.0 ± 0.5	0.5 to 0.6	165 ± 5	[10], [18]
Mo_xC_y on Mo/H-ZSM-5	13.0 to 15.0	0.8 to 1.0	280 ± 20	[10], [18]
MoO_xC_y-1[a)] on Mo/H-ZSM-5	5.3 ± 0.2	0.5 to 0.6	-84 ± 4	[18]
MoO_xC_y-2[a)] on Mo/H-ZSM-5	5.8 ± 0.2	0.4 to 0.5	-48 ± 5	[18]

a) determined by 2D ^{1}H-{^{95}Mo} PT D-HMQC NMR (excludes Mo species without protons in their vicinity)

Table 1

Catalyst preparation: Pure Mo-containing materials were utilized for ^{95}Mo solid-state NMR studies without specific treatments. The preparation procedures of Mo/H-ZSM-5 are very different and given in the references. The Mo/H-ZSM-5 zeolites used for catalysis were studied as obtained after the MDA reaction.

^{95}Mo solid-state NMR studies: The static ^{95}Mo quad-echo NMR and the ^{95}Mo MAS NMR spectra in **Fig. 1** were acquired at ν_0 = 26 MHz using a Bruker AMX-400 (B_0 = 9.4 T) spectrometer using a Bruker double-bearing MAS probe with 7 mm zirconia rotors [1]. The static ^{95}Mo WURST-QCPMG (wideband uniform-rate smooth truncation quadrupolar Carr-Purcell-Meiboom-Gill) NMR spectra in **Figs. 3 and 4** were recorded at B_0 = 18.8 T at the resonance frequency of ν_0 = 52.15 MHz, utilizing a Bruker Avance III 800 spectrometer and a 7 mm HX low frequency probe. For these spectra, 80 µs wideband WURST pulses were applied with a range of 800 kHz, and the recycle delay was 0.15 s. To record the full spectra, multiple (nine) spectra

slices were measured with an excitation frequency offset of 100 kHz and co-added [10].

The 2D ^{1}H-{^{95}Mo} PT-D-HMQC NMR spectra in **Fig. 6** were collected by using the same spectrometer and probe with a magic angle spinning rate of ν_{rot} = 40 kHz. The rf-field strength for the $\pi/2$ and π pulses in the ^{1}H channel was set to ν_{rf} = 132 kHz, which yielded $\pi/2$ and pulse lengths of 1.9 µs and 3.8 µs, respectively. The central transition selective $\pi/2$-pulse-length on the ^{95}Mo channel was 8.5 µs. The population transfers were achieved by repeatedly applying the WURST adiabatic pulses during the recoupling periods on the ^{95}Mo channel, with a duration of 98 µs, a maximal rf-field of ν_{rf} = 36 kHz, and an offset of ν_{off} = 180 kHz [10, 18].

The ^{95}Mo chemical shifts are referenced to 1.5 M aqueous alkaline solution of Na_2MoO_4 with pH = 11 (see e.g. Ref. [6]).

References:

[1] K. Eichele, R.E. Wasylishen, J.H. Nelson, *Solid-state ^{95}Mo NMR studies of some prototypal molybdenum compounds: Sodium molybdate dihydrate, hexacarbonylmolybdenum, and pentacarbonyl phosphine molybdenum(0) complexes*, J. Phys. Chem. A 1001 (1997) 5463-5468, DOI: 10.1021/jp9712415.

[2] T.J. Bastow, *^{95}Mo NMR: Hyperfine interactions in MoO_3, MoS_2, $MoSe_2$, Mo_3Se_4, $MoSi_2$ and Mo_2C*, Solid State Nucl. Magn. Reson. 12 (1998) 191-199, DOI: 10.1016/S0926-2040(98)00067-8.

[3] J.C. Edwards, R.D. Adams, P.D. Elli, *A ^{95}Mo solid-state NMR study of hydrodesulfurization catalysts. 1. Formation of fresh HDS catalyst precursors by adsorption of polyoxomolybdates onto γ-alumina*, J. Am. Chem. Soc. 112 (1990) 8349-8364, DOI: 10.1021/ja00179a020.

[4] J.C. Edwards, J. Zubieta, S.N. Shaikh, Q. Chen, S. Bank, P.D. Ellis, *Solid-state ^{95}Mo NMR study of (aryldiazenido)- and (organohydrazido) polyoxomolybdates. Investigation of model compounds of catalytic molybdenum environments*, Inorg. Chem. 29 (1990) 3381-3393, DOI: 10.1021/ic00343a024.

[5] D.L. Bryce, R.E. Wasylishen, *A ^{95}Mo and ^{13}C solid-state NMR and relativistic DFT investigation of mesitylenetricarbonylmolybdenum(0) - a typical transition metal piano-stool complex*, Phys. Chem. Chem. Phys. 4 (2002) 3591-3600, DOI: 10.1039/b202025b.

[6] J.-B. d'Espinose de Lacaillerie, F. Barberon, K.V. Romanenko, O.B. Lapina, L. Le Polles, R. Gautier, Z. Gan, *^{95}Mo magic angle spinning NMR at high field: Improved measurements and structural analysis of the quadrupole interaction in monomolybdates and isopolymolybdates*, J. Phys. Chem. B 109 (2005) 14033-14042, DOI: 10.1021/jp0519621.

[7] M.A.M. Forgeron, R.E. Wasylishen, *A solid-state ^{95}Mo NMR and computational investigation of dodecahedral and square antiprismatic octacyanomolybdate(IV) anions: Is the point-charge approximation an accurate probe of local symmetry?*, J. Am. Chem. Soc. 128 (2006) 7817-7827, DOI: 10.1021/ja060124x.

[8] Z.J. Berkson, R. Zhu, C. Ehinger, L. Lätsch, S.P. Schmid, D. Nater, S. Pollitt, O.V. Safonova, S. Björgvinsdóttir, A.B. Barnes, Y. Román-Leshkov, G.A. Price, G.J. Sunley, C. Copéret, *Active site descriptors from ^{95}Mo NMR signatures of silica supported Mo-based olefin metathesis catalysts*, J. Am. Chem. Soc. 145 (2023) 12651-12662, DOI: 10.1021/jacs.3c02201.

[9] W. Gao, G. Qi, Q. Wang, W. Wang, S. Li, I. Hung, Z. Gan, J. Xu, F. Deng, *Dual active sites on molybdenum/ZSM-5 catalyst for methane dehydroaromatization: Insights from solid-state NMR spectroscopy*, Angew. Chem. Int. Ed. 60 (2021) 10709-10715, DOI: 10.1002/anie.202017074.

[10] W. Gao, Q. Wang, G. Qi, J. Liang, C. Wang, J. Xu, F. Deng, *Active ensembles in methane dehydroaromatization over molybdenum/ZSM-5 zeolite identified by 2D ^{1}H ^{95}Mo magic angle spinning nuclear magnetic resonance correlation spectroscopy*, Angew. Chem. Int. Ed. 62 (2023) e202306133, DOI: 10.1002/anie.202306133.

[11] F.H. Larsen, H.J. Jakobsen, P.D. Ellis, N.C. Nielsen, *Sensitivity-enhanced quadrupolar-echo NMR of half-integer quadrupolar nuclei. Magnitudes and relative orientation of chemical shielding and quadrupolar coupling tensors*, J. Phys. Chem. A 101 (1997) 8597-8606, DOI: 10.1021/jp971547b.

[12] I. Hung, Z. Gan, *On the practical aspects of recording wideline QCPMG NMR spectra*, J. Magn. Reson. 204 (2010) 256-265, DOI: 10.1016/j.jmr.2010.03.001.

[13] L.A. O'Dell, R.W. Schurko, *QCPMG using adiabatic pulses for faster acquisition of ultra-wideline NMR spectra*, Chem. Phys. Lett. 464 (2008) 97-102, DOI: 10.1016/j.cplett.2008.08.095.

[14] L.A. O'Dell, A.J. Rossini, R.W. Schurko, *Acquisition of ultra-wideline NMR spectra from quadrupolar nuclei by frequency stepped WURST–QCPMG*, Chem. Phys. Lett. 468 (2009) 330–335, DOI: 10.1016/j.cplett.2008.12.044.

[15] H. Zheng, D. Ma, X. Bao, J.Z. Hu, J.H. Kwak, Y. Wang, C.H. F. Peden, *Direct observation of the active center for methane dehydroaromatization using an ultrahigh field ^{95}Mo NMR spectroscopy*, J. Am. Chem. Soc. 130 (2008) 3722-3723, DOI: 10.1021/ja7110916.

[16] J.Z. Hu, J.H. Kwak, Y. Wang, C.H.F. Peden, H. Zheng, D. Ma, X. Bao, *Studies of the active sites for methane dehydroaromatization using ultrahigh-field solid-state ^{95}Mo NMR spectroscopy*, J. Phys. Chem. C 113 (2009) 2936-2942, DOI: 10.1021/jp8107914.

[17] C.H.L. Tempelman, V.O. de Rodriguesa, E.R.H. van Eck, P.C.M.M. Magusin, E.J.M. Hensen, *Desilication and silylation of Mo/HZSM-5 for methane dehydroaromatization*, Microporous Mesoporous Mater. 203 (2015) 259-273, DOI: 10.1016/j.micromeso.2014.10.020.

[18] W. Gao, G. Qi, C. Wang, Q. Wang, J. Liang, J. Xu, F. Deng, *Molybdenum/ZSM-5 catalyzes methane co-aromatization with furan: Unveiling the mechanism with solid-state NMR*, ACS Catal. 14 (2024) 8220-8231, DOI: 10.1021/acscatal.4c01827.

[19] Q. Wang, J. Trebosc, Y. Li, J. Xu, B. Hu, N. Feng, Q. Chen, O. Lafon, J.P. Amoureux, F. Deng, *Signal enhancement of J-HMQC experiments in solid-state NMR involving half-integer quadrupolar nuclei*, Chem. Commun. 49(59) (2013) 6653-6655, DOI: 10.1039/c3cc42961j.

[20] Q. Wang, Y. Li, J. Trebosc, O. Lafon, J. Xu, B. Hu, N. Feng, Q. Chen, J.P. Amoureux, F. Deng, *Population transfer HMQC for half-integer quadrupolar nuclei*, J. Chem. Phys. 142(9) (2015) 094201, DOI: 10.1063/1.4913683.